magnetochemistry

MDPI

Article

Structure and Magnetic Properties of the Spin Crossover Linear Trinuclear Complex $[Fe_3(furtrz)_6(ptol)_2(MeOH)_4]\cdot 4(ptol)\cdot 4(MeOH)$ (furtrz: furanylidene-4H-1,2,4-triazol-4-amine ptol: *p*-tolylsulfonate)

Y. Maximilian Klein [1], Natasha F. Sciortino [2], Catherine E. Housecroft [1], Cameron J. Kepert [2] and Suzanne M. Neville [2,*]

1 Department of Chemistry, University of Basel, Spitalstrasse 51, Basel, CH-4056, Switzerland; max.klein@unibas.ch (Y.M.K.); catherine.housecroft@unibas.ch (C.E.H.)

2 School of Chemistry, The University of Sydney, New South Wales 2006, Australia; natasha.sciortino@sydney.edu.au (N.F.S.); cameron.kepert@sydney.edu.au (C.J.K.)

* Correspondence: suzanne.neville@sydney.edu.au; Tel.: +61-2-9351-7791; Fax: +61-2-9351-3329

Academic Editors: Guillem Aromí and José Antonio Real

Received: 15 January 2016; Accepted: 2 February 2016; Published: 16 February 2016

Abstract: The furan-functionalised 1,2,4-triazole ligand furanylidene-4H-1,2,4-triazol-4-amine (furtrz) has been incorporated into the trinuclear complex $Fe_3(furtrz)_6(ptol)_2(MeOH)_4]\cdot 4(ptol)\cdot 4(MeOH)$ (ptol = *p*-tolylsulfonate) composed of $\mu_{1,2}$-triazole bridges between iron(II) sites, as per one-dimensional chain materials, and terminally coordinated ptol anions and methanol molecules. Magnetic susceptibility measurements reveal a gradual single-step spin crossover (SCO) behavior of one third of the iron(II) sites per trinuclear unit. Single-crystal X-ray diffraction below the transition (90 K) shows the central iron(II) sites undergo a HS to LS transition and the peripheral ones remain HS (HS = high spin; LS = low spin). This is a rare example of a cationic trinuclear SCO material where the discrete unit includes bound anions.

Keywords: spin-crossover; iron(II); trinuclear; crystal structure; magnetism; 1,2,4-triazole

1. Introduction

In the expanding field of spin crossover (SCO) complex synthesis and characterization, mononuclear and polymeric materials are most commonly reported [1–3]. The relatively fewer reports dealing with discrete polynuclear complexes, *i.e.*, those with two or more interconnected SCO-active sites, is largely due to the significant synthetic challenges involved in their design, successful synthesis and eventual SCO properties [4–13]. In particular, SCO properties are difficult to predict because solid state interactions (such as hydrogen-bonding and π-stacking), which partially govern the presence or absence of SCO and the SCO character attained, are difficult to control in the targeted preparation of discrete supramolecular species [14]. Thus the successful preparation and analysis of novel discrete SCO materials is important, including the expansion of existing families such that trends can be extracted for future reference.

Several trinuclear SCO materials have been reported, composed of the linear arrangement of iron(II) sites bridged by 1,2,4-triazole-type ligands of various 4-functionalisation [15–18]. These materials are particularly useful as a tool for modelling the SCO behavior of one-dimensional 1,2,4-triazole ligand chain materials as the central iron(II) sites are of the same $[FeN_6]$ coordination environment [19,20]. The peripheral iron(II) sites are most commonly terminally coordinated by

water (or other solvent) molecules which prevent polymeric formation. Within this general family of trinuclear materials a range of gradual and abrupt SCO behaviors have been reported depending on the functional group of the 1,2,4-triazole ligand, the charge balancing anion and degree of lattice solvation. For example, $[Fe_3(hyetrz)_6(H_2O)_6](CF_3SO_3)_6$ (hyetrz = 4-(2′-hydroxyethyl)-1,2,4-triazole) displays a gradual SCO centred at room temperature [17] and the partially dehydrated material $[Fe_3(\mu\text{-}L)_6(H_2O)_6]\cdot 5H_2O$ (*L* = 4-(1,2,4-triazol-4-yl)ethanesulfonate) shows a hysteretic transition above room temperature ($T_{½}\uparrow\downarrow$357, 343 K) [18]. We report here the structure and magnetism of a SCO trinuclear material in which the terminal iron(II) sites are capped by both solvent and bound anions, for which there are few examples.

2. Results and Discussion

2.1. Synthesis and Characterisation

The new ligand furtrz was prepared by the condensation reaction of 4-amino-4H-1,2,4-triazole and 2-furfural (Figure 1). Single crystals of $[Fe_3(furtrz)_6(ptol)_2(MeOH)_4]\cdot 4(ptol)\cdot 4(MeOH)$ were formed overnight in a methanolic solution of the iron(II) p-tolylsulfonate salt and furtrz ligand. The yellow crystals turn purple in liquid nitrogen indicating the presence of a SCO.

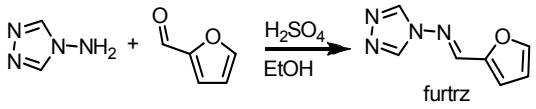

Figure 1. Synthetic scheme to prepare the furtrz ligand.

2.2. Magnetic Susceptibility Measurements

Temperature dependent magnetic susceptibility measurements on a bulk crystalline sample of $[Fe_3(furtrz)_6(ptol)_2(MeOH)_4]\cdot 4(ptol)\cdot 4(MeOH)$ revealed a gradual one-step SCO (Figure 2). At 300 K, the $\chi_M T$ values of 10.2 cm·K·mol^{-1} are consistent with all iron(II) sites being in the HS state per trinuclear domain. These values remain approximately constant until 200 K where there is a gradual decrease in $\chi_M T$ values to 7.8 cm·K·mol^{-1} by 50 K. The $\chi_M T$ values at 50 K indicate of a SCO of one-third of the iron(II) sites to the LS state. No thermal hysteresis was observed with heating.

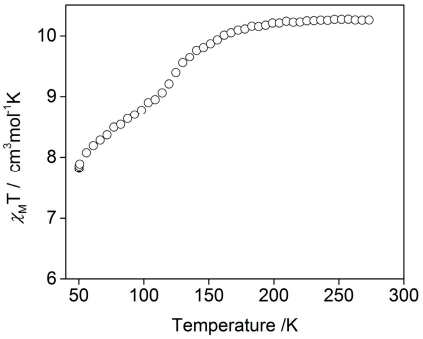

Figure 2. χ_MT versus temperature for $[Fe_3(furtrz)_6(ptol)_2(MeOH)_4]\cdot 4(ptol)\cdot 4(MeOH)$.

2.3. Structural Characterisation

Single crystal X-ray diffraction data were collected at 90 K; an atomic displacement ellipsoid plot is shown in Figure 3 and relevant bond length, angle and interaction information are given in Tables 1 and 2. This material crystallises in the triclinic space group *P*-1. In each trinuclear unit the iron(II) sites are arranged in a linear fashion bridged by triazole groups from the furtrz ligands (Figure 4). The central iron(II) site, Fe1, is in an octahedral $[FeN_6]$ coordination environment and sits on an inversion centre such that there are only two unique metal centres per trinuclear unit, Fe1 and

Fe2. The outer iron(II) sites, Fe2 and Fe2′, are in a $[FeN_3O_3]$ coordination environment owing to the coordination of two methanol solvent molecules and one *p*-tolylsulfonate anion (Figure 4). All of the furtrz ligand are in a *cis*-orientation with respect to the furan oxygen and imine nitrogen atoms. Each trinuclear unit is cationic with a 4+ charge which is balanced by four unbound *p*-tolylsulfonate anions alongside four lattice methanol molecules. Thus, the overall formula per trinuclear species is $[Fe_3(furtrz)_6(ptol)_2(MeOH)_4]\cdot 4(ptol)\cdot 4(MeOH)$.

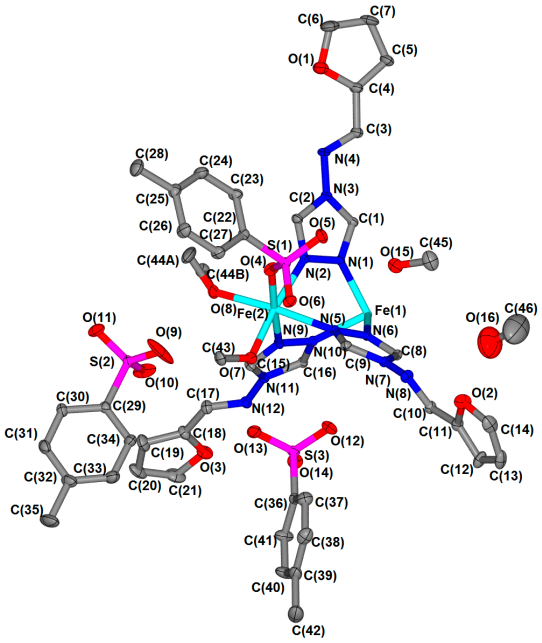

Figure 3. Thermal ellipsoid representation (50% probability) of the crystal structure at 90 K. Hydrogen atoms omitted for clarity.

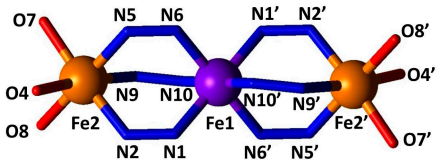

Figure 4. Direct coordination environment of iron(II) sites with labels. Iron(II) sites (spheres) are coloured according to spin state (high spin (HS): orange, low spin (LS): purple).

Table 1. Selected single crystal structural parameters at 90 K.

Bond	/Å	Angle	/°
Fe1–N1	2.0274(18)	N1–Fe1–N6	91.65(7)
Fe1–N6	2.0131(17)	N1–Fe1–N10	91.91(7)
Fe1–N10	2.0169(18)	N6–Fe1–N10	91.46(7)
Fe2–N2	2.1366(18)	N2–Fe2–N5	85.85(7)
Fe2–N5	2.1260(18)	N2–Fe2–N9	87.48(7)
Fe2–N9	2.1789(18)	N5–Fe2–N9	86.78(7)
Fe2–O4	2.1066(17)	N2–Fe2–O4	86.53(7)
Fe2–O7	2.0872(16)	N2–Fe2–O8	96.82(7)
Fe2–O8	2.0995(17)	N5–Fe2–O4	94.13(7)
-	-	N5–Fe2–O7	87.96(7)
-	-	N9–Fe2–O7	94.67(7)
-	-	N9–Fe2–O8	88.97(8)
-	-	O4–Fe2–O7	91.42(7)
-	-	O4–Fe2–O8	90.41(8)
-	-	O7–Fe2–O8	89.54(7)

Table 2. Inter- and intramolecular interactions and other parameters.

Interactions	/Å
Intramolecular	-
O6 ... C9	3.200(2)
Intermolecular interactions (trinuclear ... trinuclear)	-
O1 ... C19_$1	3.444(2)
N12 ... C6_$2	3.488(3)
Intermolecular interactions (trinuclear ... free anion)	-
C17 ... O10	3.074(2)
C3 ... O14	3.194(4)
C8 ... O11_$3	3.024(4)
C1 ... O12_$4	3.288(6)
Intermolecular interactions (bound anion ... solvent)	-
O5 ... O15	2.817(2)
Intermolecular interactions (free anion ... solvent)	-
O9 ... O7	3.247(4)
O13 ... O7	2.628(4)
π-stacking furan ring	-
O3 ring centroid ... centroid	3.553
Ligand torsion angles	/°
Ligand O1	21.0
Ligand O2	58.5
Ligand O3	20.8

Symmetry operators—$1: 1−x, −y, −z; $2: x,1+y,z; $3: x−1,y,z, $4: −x, −y, −z.

Of the two crystallographically unique iron(II) sites per trinuclear unit, only the central one (Fe1) is in the expected coordination environment for SCO to occur. The crystal structure determination was conducted at 90 K, below the SCO transition observed by magnetic susceptibility (Figure 2), and examination of the Fe1–N distances reveal bond lengths of approximately 2.0 Å (Table 1, Figures 3 and 4) which are consistent with this site being in the LS state at this temperature (Figure 5). The Fe2–N bond distances of approximately 2.2 Å are consistent with a HS state as expected for this coordination environment (Table 1, Figures 3 and 4).

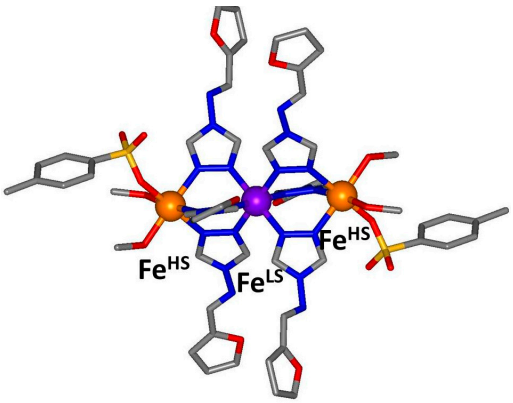

Figure 5. Structural representation of one trinuclear discrete unit at 90 K showing the HS and LS iron(II) sites. Unbound anion and solvent molecules not shown. Iron(II) sites (spheres) are coloured according to spin state at 90 K (HS: orange, LS: purple).

The crystal packing environment is largely determined by networks of intra- and inter-molecular interactions involving the sulfonate oxygen atoms of both the bound and unbound *p*-tolylsulfonate anions (Figure 6a). A comprehensive list of interactions is shown in Table 2. There is one intramolecular interaction involving a triazole group and a sulfonate oxygen (shown as green dotted lines in Figure 6a).

There are extensive intermolecular interactions involving the free *p*-tolylsulfonate anions and either the furtrz ligand imine group or the bound methanol molecules as depicted in Figure 6a (black dotted lines). The trinuclear units are packed around the edge of the unit cell with weak π-interactions between adjacent discrete units (Figure 6b region of π-stacking indicated by black circles). The centre of the unit cell is filled with free *p*-tolylsulfonate anions which run in 1-D chains along the *a*-axis with edge-to-face π-stacking interactions along the chain (shown in green in Figure 6b). Of the three crystallographically unique furtrz ligands, one is significantly less planar (i.e. more twisted with respect to the triazole and furan rings) compared to the other two (the furtrz ligand containing O2); this is to avoid a steric clash between the adjacent furan rings.

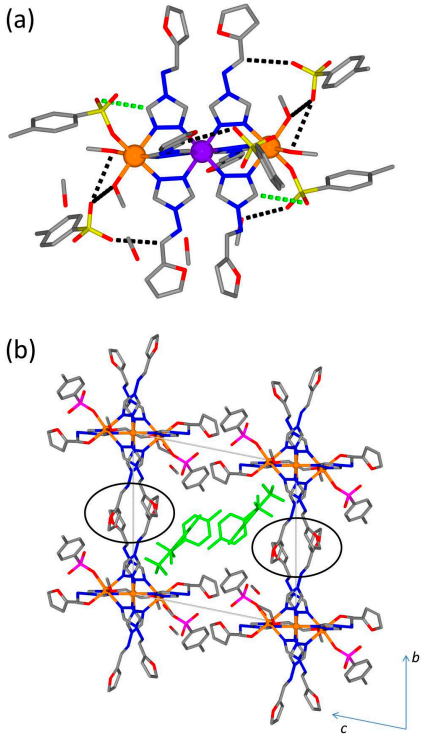

Figure 6. (**a**) Example hydrogen bonding interactions involving the sulfonate oxygen atoms (dotted lines, intramolecular interactions shown in green and intermolecular interactions shown in black, full list given in Table 2); (**b**) Packing of one unit cell highlighting the position of the free tosylate anions. Region of π-stacking interactions between adjacent trinuclear units indicated by black circles.

The overall gradual SCO behavior of this material suggests weak cooperativity between molecules in the lattice. While structural analysis revealed a dense network of intramolecular interactions, the molecular species are well separated due to the bulky aromatic substituents on the furtrz ligands and the presence of many aromatic anions, meaning the communication between SCO units would be weak [16]. Furthermore, the relatively low spin transition temperature of this material is consistent with other polymeric species which contain bulky aromatic 1,2,4-triazole ligands, thought to contribute a lower overall ligand field strength [16,21].

3. Experimental Section

3.1. Synthesis of furanylidene-4H-1,2,4-triazol-4-amine (furtrz)

In a 100 mL round-bottomed flask, with condenser 2-furfural (2.06 g, 28.5 mmol, 1.20 eq.) and 4-amino-1,2,4-triazole (2 g, 23.7 mmol, 1.00 eq.) were dissolved in EtOH (50 mL). 2 drops of sulfuric acid were added to catalyse the condensation reaction. The reaction mixture was refluxed for 5 h at 80 °C. Upon cooling the reaction mixture to room temperature, a precipitate formed, that was filtered

and washed with water (2 × 15 mL) and ethanol (2 × 15 mL) to give an off-white powder. The powder was dissolved in MeCN (50 mL) and filtered over SiO_2 to remove impurities. The solvent was removed *in vacuo* and the solid recrystallized from EtOH. The triazole- ligand furtrz (2.67 g, 16.5 mmol, 69.4%) was obtained as a white powder. **^{1}H-NMR** (500 MHz, MeOD-d_4, δ/ppm, Figure 7): 8.99 (s, 2H, **1**), 8.83 (s, 1H, **2**), 7.84 (d, $^3J_{HH}$ = 7.6 Hz, 1H, **6**), 7.21 (d, $^3J_{HH}$ = 3.5 Hz, 1H, **4**), 6.70 (d, $^4J_{HH}$ = 1.5 Hz, 1H, **5**). **^{13}C-NMR** (126 MHz, MeOD-d_4, δ/ppm): 149.15 ($C^{6/6'}$), 152.56 (C^3), 148.77 (C^6), 148.60 (C^2), 140.32 (C^1), 120.37 (C^4), 113.82 (C^5). **IR** (solid, v/cm^{-1}): 3120 (m), 3018 (w), 2968 (w), 2908 (w), 2672 (w), 2380 (w), 2104 (w), 1727 (w), 1619 (m), 1510 (s), 1487 (s), 1457 (w), 1397 (w), 1372 (w), 1322 (w), 1303 (m), 1225 (w), 1168 (s), 1059 (s), 1024 (s), 964 (m), 942 (s), 882 (m), 838 (m), 763 (m), 696 (w), 670 (w), 613 (w). Elemental analysis calcd. (%) for $N_4C_7OH_6$ (162.15) C 51.85, H 3.73, N 34.55; found: C 51.0, H 3.8, N 34.8.

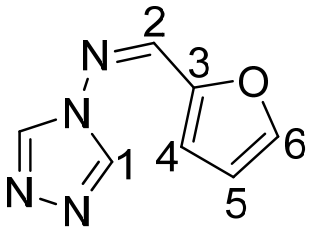

Figure 7. furanylidene-4H-1,2,4-triazol-4-amine (furtrz).

3.2. Synthesis of [Fe$_3$(furtrz)$_6$(ptol)$_2$(MeOH)$_4$]· 4(ptol)· 4(MeOH)

[Fe(H_2O)$_6$](ptol)$_2$ (147.74 mg, 0.371 mmol) was dissolved in MeOH (3–5 mL), a few drops of water and a spatula-tip of ascorbic acid were added. This solution was then added to a second vial, containing a furtrz (200.0 mg, 1.235 mmol) solution in MeOH (3–5 mL). The yellow solution was allowed to stand for 3 days in the closed vial and after that period yellow crystals were obtained at the wall of the vial. **IR** (solid, v/cm^{-1}): 3159 (m), 3095 (m), 2992 (w), 1616 (m), 1533 (m), 1471 (m), 1399 (w), 1375 (w), 1322 (w), 1290 (w), 1221 (s), **1180** (s), 1122 (s), 1068 (m), 1034 (s), 1010 (s), 996 (w), 939 (w), 884 (w), 815 (m), 774 (m), 684 (s), **622** (w), 592 (w).

3.3. Magnetic Measurements

Solid state magnetic susceptibility data were collected on a Quantum Design Versalab System with a Vibrating Sample Magnetometer attachment. The sample was loaded into a polyethylene sample container, under a small layer of diffusion solvent and sealed with Teflon tape. Measurements were taken continuously with a ramp rate of 2 K min^{-1} (no overshoot) under a field of 0.3 T, in the range 300 ↔ 50 K.

3.4. Single Crystal Diffraction

Single crystal X-ray diffraction data was collected on an Agilent SuperNova Dual Source diffractometer employing a Mo-K$_\alpha$ radiation source (λ = 0.71073 Å). An Oxford Cryosystems Cryostream attachment produced a continuous stream of dry dinitrogen and facilitated temperature control. Crystals obtained from the diffusions were coated in a thin film of paratone-N oil and mounted on a loop. Data integration and reduction were performed using CrysAlisPro [22] for the SupaNova collection. Subsequent computations were performed with the X-Seed graphical user interface [22,23]. All crystal structures were solved by direct methods using SHELX-97 and refined within SHELXL-97 [24]. All atoms were refined anisotropically and hydrogen atoms were fixed using the riding model. A summary of the crystallographic and refinement details are presented in Table 3. CCDC-1442227 contain the supplementary crystallographic data for this paper. These data can be obtained free of charge from the Cambridge Crystallographic Data Centre via www.ccdc.cam.ac.uk/data_request/cif.

Table 3. Single crystal diffraction refinement parameters.

Temperature [K]	**90**
Formula	$C_{92}H_{80}Fe_3N_{24}O_{32}S_6$
Formula weight [g·mol^{-1}]	2393.71
Crystal system	Triclinic
Space group	*P*-1
a [Å]	12.0480(4)
b [Å]	15.1401(5)
c [Å]	16.3117(5)
α [°]	96.793(3)
β [°]	109.986(3)
γ [°]	100.624(3)
V [Å^3]	2694.80(15)
D_c [Mg m^{-3}]	1.508
Data/restraints/parameters	18122/0/177
$R(F)$ ($I > \sigma(I)$, all)	0.0537, 0.0790
$R_w(F^2)$ ($I > 2\sigma(I)$, all)	0.1364, 0.1568
GoF	0.946

4. Conclusions

The material $[Fe_3(furtrz)_6(ptol)_2(MeOH)_4]\cdot 4(ptol)\cdot 4(MeOH)$ is a new addition to the trinuclear SCO family. Magnetic susceptibility and structural measurements reveal a HS to LS transition of the central iron(II) site. This trinuclear material contains the rare binding of terminal anions on the peripheral iron(II) sites. The crystal packing is dominated by interaction involving both the bound and unbound anions indicating that this material may be stable for lattice solvent removal or exchange, which has been shown in other such materials to alter the SCO properties. Preparation of trinuclear materials incorporating the furtrz ligand but with an anion that has less aromatic and hydrogen bonding capacity in the future would be useful in assessing the impact of these characteristics on SCO behavior.

Acknowledgments: The Australian Research Council is thanked for providing Discovery Grants and Research Fellowships to support this work at the University of Sydney and for supporting Y. Maximilian Klein during an international Masters project from the University of Basel.

Author Contributions: Synthesis and characterization was conducted by Y. Maximilian Klein. Single-crystal X-ray diffraction data collection and refinement and magnetic measurements were carried out by Y. Maximilian Klein, Natasha F. Sciortino and Suzanne M. Neville. The manuscript was prepared and edited by Catherine E. Housecroft, Cameron J. Kepert and Suzanne M. Neville.

Conflicts of Interest: The authors declare no conflict of interest.

References

1. Gütlich, P.; Goodwin, H.A. Spin crossover—An overall perspective. *Top. Curr. Chem.* **2004**, *233–235*, 1–47.
2. Gütlich, P.; Gaspar, A.B.; Garcia, Y. Spin state switching in iron coordination compounds. *Beilstein J. Org. Chem.* **2013**, *9*, 342–391. [CrossRef] [PubMed]
3. Halcrow, M.A. *Spin-Crossover Materials: Properties and Applications*; John Wiley & Sons, Ltd.: Oxford, UK, 2013.
4. Bousseksou, A.; Molnár, G.; Real, J.A.; Tanaka, K. Spin crossover and photomagnetism in dinuclear iron(II) compounds. *Coord. Chem. Rev.* **2007**, *251*, 1822–1833. [CrossRef]
5. Olguín, J.; Brooker, S. *Spin-Crossover in Discrete Polynuclear Complexes, in Spin-Crossover Materials: Properties and Applications*; John Wiley & Sons, Ltd.: Oxford, UK, 2013.
6. Neville, S.M. Metallosupramolecular materials for magnetic applications: Spin-crossover. In *Functional Metallosupramolecular Materials*; Hardy, G.J., Schacher, F.H., Eds.; Royal Society of Chemistry: Cambridge, UK, 2015; pp. 290–317.

7. Ren, D.-H.; Qiu, D.; Pang, C.Y.; Li, Z.; Gu, Z.-G. Chiral tetrahedral iron(II) cages: Diastereoselective subcomponent self-assembly, structure interconversion and spin-crossover properties. *Chem. Commun.* **2015**, *51*, 788–791. [CrossRef] [PubMed]
8. Duriska, M.B.; Neville, S.M.; Moubaraki, B.; Cashion, J.D.; Halder, G.J.; Chapman, K.W.; Baldé, C.; Létard, J.-F.; Murray, K.S.; Kepert, C.J.; *et al*. A Nanoscale Molecular Switch Triggered by Thermal, Light, and Guest Perturbation. *Angew. Chem. Int. Ed.* **2009**, *48*, 2549–2552. [CrossRef] [PubMed]
9. Steinert, M.; Schneider, B.; Dechert, S.; Demeshko, S.; Meyer, F. A trinuclear defect-grid iron(II) spin crossover complex with a large hysteresis loop that is readily silenced by solvent vapor. *Angew. Chem. Int. Ed.* **2014**, *53*, 6135–6139. [CrossRef] [PubMed]
10. Bilbeisi, R.A.; Zarra, S.; Feltham, H.L.C.; Jameson, G.N.L.; Clegg, J.K.; Brooker, S.; Nitschke, J.R. Guest Binding Subtly Influences Spin Crossover in an $Fe^{II}{}_4L_4$ Capsule. *Chem. Eur. J.* **2013**, *19*, 8058–8062. [CrossRef] [PubMed]
11. Ferguson, A.; Squire, M.A.; Siretanu, D.; Mitcov, D.; Mathonière, C.; Clérac, R.; Kruger, P.E. A face-capped $[Fe_4L_4]_8{}^+$ spin crossover tetrahedral cage. *Chem. Commun.* **2013**, *49*, 1597–1599. [CrossRef] [PubMed]
12. Hietsoi, O.; Dunk, P.W.; Stout, H.D.; Arroyave, A.; Kovnir, K.; Irons, R.E.; Kassenova, N.; Erkasov, R.; Achim, C.; Shartruk, M. Spin crossover in tetranuclear Fe(II) complexes, {(tpma)Fe(*m*-CN)$_4$}X_4 (X = $ClO_4{}^-$, $BF_4{}^-$). *Inorg. Chem.* **2014**, *53*, 13070–13077. [CrossRef] [PubMed]
13. Matsumoto, T.; Newton, G.N.; Shiga, T.; Hayami, S.; Matsui, Y.; Okamoto, H.; Kumai, R.; Murakami, Y.; Oshio, H. Programmable spin-state switching in a mixed-valence spin-crossover iron grid. *Nat. Commun.* **2014**, *5*, 3865–3873. [CrossRef] [PubMed]
14. Halcrow, M.A. Structure:function relationships in molecular spin-crossover complexes. *Chem. Soc. Rev.* **2011**, *40*, 4119–4142. [CrossRef] [PubMed]
15. Thomann, M.; Kahn, O.; Guilhem, J.; Varret, F. Spin Conversion *versus* Antiferromagnetic Interaction in Iron(II) Trinuclear Species. Crystal Structures and Magnetic Properties of $[Fe_3(p\text{-MeOptrz})_6(H_2O)_4](BF_4)_6$ and $[Fe_3(p\text{-MeOptrz})_6(H_2O)_6](tos)_6$ [p-MeOptrz = 4-*p*-Methoxyphenyl)-1,2,4-triazole, tos =Tosylate]. *Inorg. Chem.* **1994**, *33*, 6029–6037.
16. Savard, D.; Cook, C.; Enright, G.D.; Korobkov, I.; Burchell, T.J.; Murugesu, M. Gradual spin crossover behaviour in a linear trinuclear Fe^{II} complex. *Cryst. Eng. Commun.* **2011**, *13*, 5190–5197. [CrossRef]
17. Garcia, Y.; Guionneau, P.; Bravic, G.; Chasseau, D.; Howard, J.A.K.; Kahn, O.; Ksenofontov, V.; Reiman, S.; Gütlich, P. Synthesis, Crystal Structure, Magnetic Properties and ^{57}Fe Mössbauer Spectroscopy of the New Trinuclear $[Fe_3(4\text{-}(2'\text{-hydroxyethyl})\text{-}1,2,4\text{-triazole})_6(H_2O)_6](CF_3SO_3)_6$ Spin Crossover Compound. *Eur. J. Inorg. Chem.* **2000**, *2000*, 1531–1538. [CrossRef]
18. Gómez, V.; Benet-Buchholz, J.; Martin, E.; Galán-Mascarós, J.R. Hysteretic Spin Crossover above Room Temperature and Magnetic Coupling in Trinuclear Transition-Metal Complexes with Anionic 1,2,4-Triazole Ligands. *Chem. Eur. J.* **2014**, *20*, 5369–5379. [CrossRef] [PubMed]
19. Grosjean, A.; Négrier, P.; Bordet, P.; Etrillard, C.; Mondieig, D.; Pechev, S.; Lebraud, E.; Létard, J.-F.; Guionneau, P. Crystal Structures and Spin Crossover in the Polymeric Material $[Fe(Htrz)_2(trz)](BF_4)$ Including Coherent-Domain Size Reduction Effects. *Eur. J. Inorg. Chem.* **2013**, *2013*, 796–802. [CrossRef]
20. Roubeau, O. Triazole-Based One-Dimensional Spin-Crossover Coordination Polymers. *Chem. Eur. J.* **2012**, *18*, 15230–15244. [CrossRef] [PubMed]
21. Roubeau, O.; Gamez, P.; Teat, S.J. Dinuclear Complexes with a Triple N1,N2-Triazole Bridge that Exhibit Partial Spin Crossover and Weak Antiferromagnetic Interactions. *Eur. J. Inorg. Chem.* **2013**, *2013*, 934–942. [CrossRef]
22. *CrysAlisPro, V1.171.136.128*; Agilent Technologies: Yarnton, Oxfordshire, England, 2013.
23. Barbour, L.J. X-Seed—A software tool for supramolecular crystallography. *J. Supramol. Chem.* **2001**, *1*, 189–191. [CrossRef]
24. Sheldrick, G.M. A short history of SHELX. *Acta Crystallogr. Sec. A* **2008**, *64*, 112–122. [CrossRef] [PubMed]